Supplementary Materials

Sulfur-Doped Graphdiyne as a High-Capacity Anode Material for Lithium-Ion Batteries

Fanan Kong, Yong Yue, Qingyin Li, and Shijie Ren *

State Key Laboratory of Polymer Materials Engineering, College of Polymer Science and Engineering, Sichuan University, Chengdu 610065, China
* Correspondence: rensj@scu.edu.cn

Contents

Section 1. NMR spectrum of the monomers

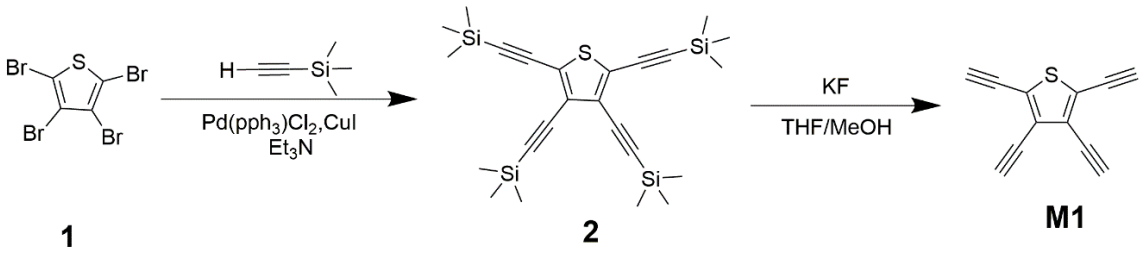

Figure S1. Synthesis of 2,3,4,5-tetrakis[(trimethylsilyl)ethynyl]-thiophene (**2**) and 2,3,4,5-tetraethynyl thiophene (**M1**).

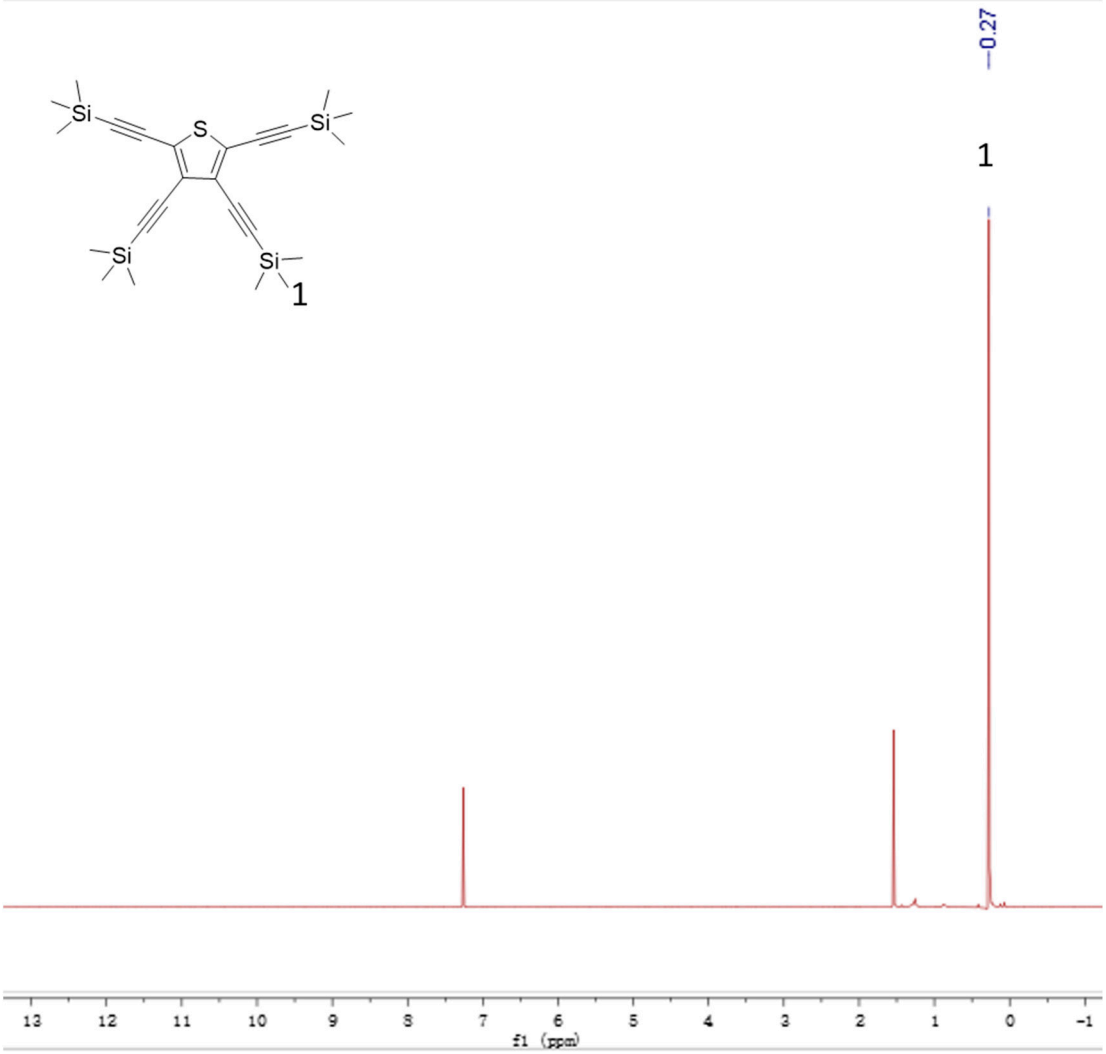

Figure S2. ^{1}H NMR spectrum of 2,3,4,5-tetrakis[(trimethylsilyl)ethynyl]-thiophene (**2**).

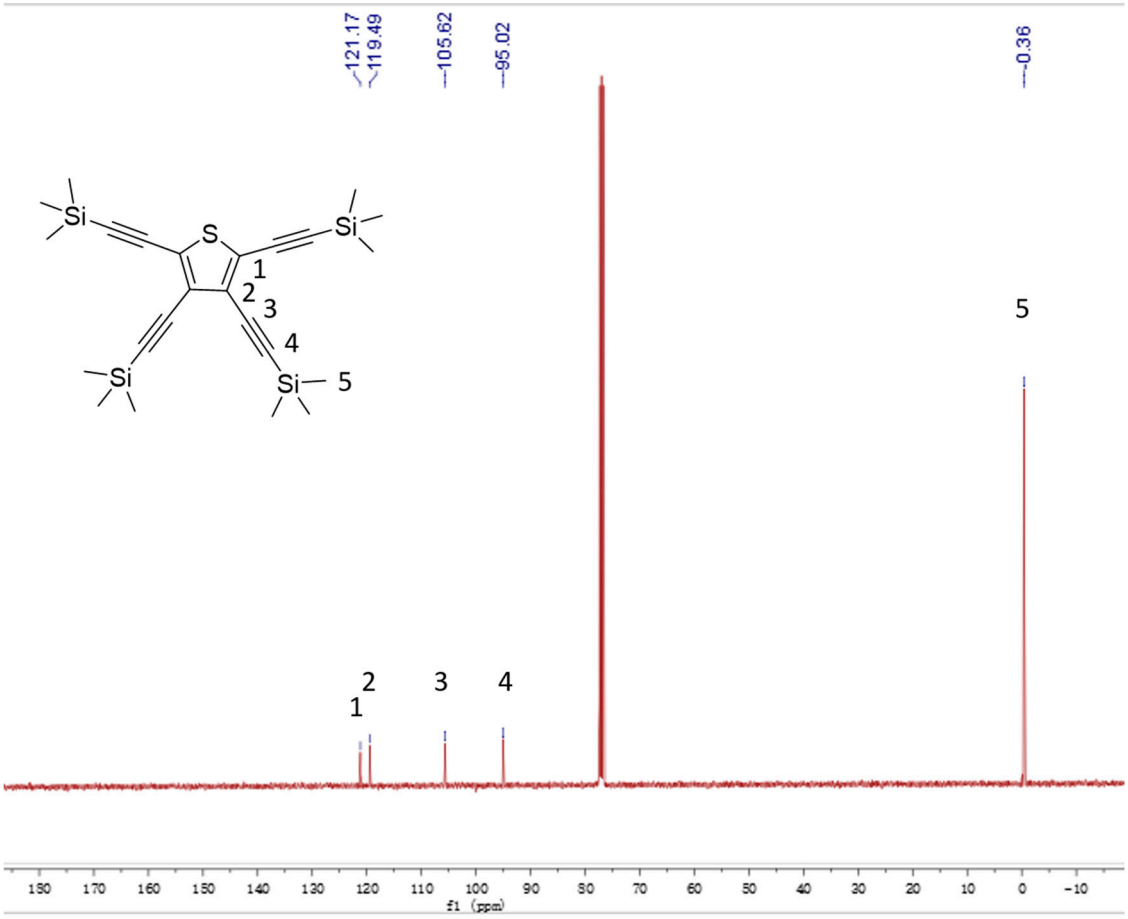

Figure S3. ^{13}C NMR spectrum of 2,3,4,5-tetrakis[(trimethylsilyl)ethynyl]-thiophene (**2**).

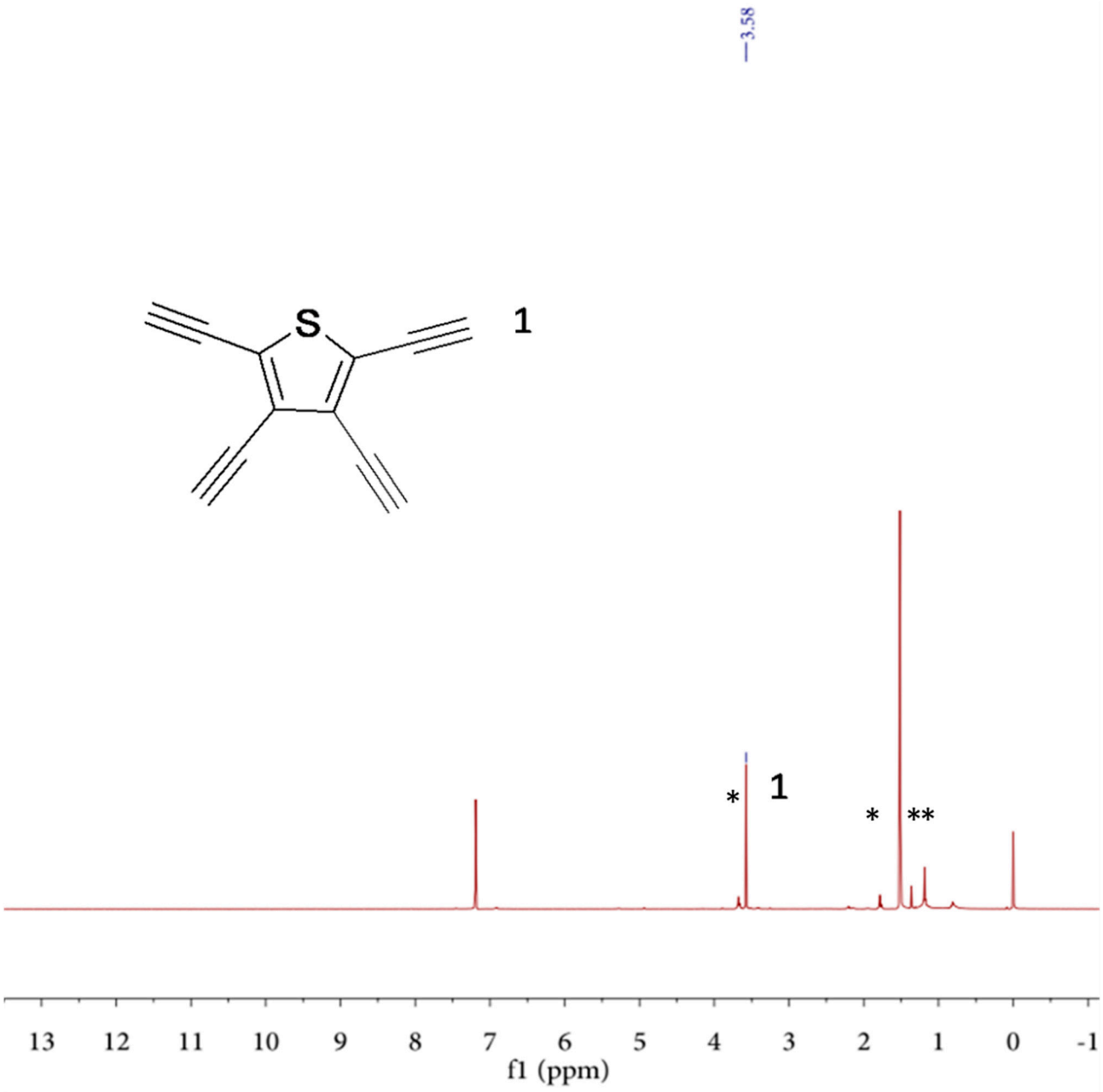

Figure S4. ^{1}H NMR spectrum of 2,3,4,5-tetraethynyl thiophene (**M1**). Attention: The NMR will be done immediately after the rotary evaporation since the monomer is unstable in the air. * may be caused by some residual solvent.

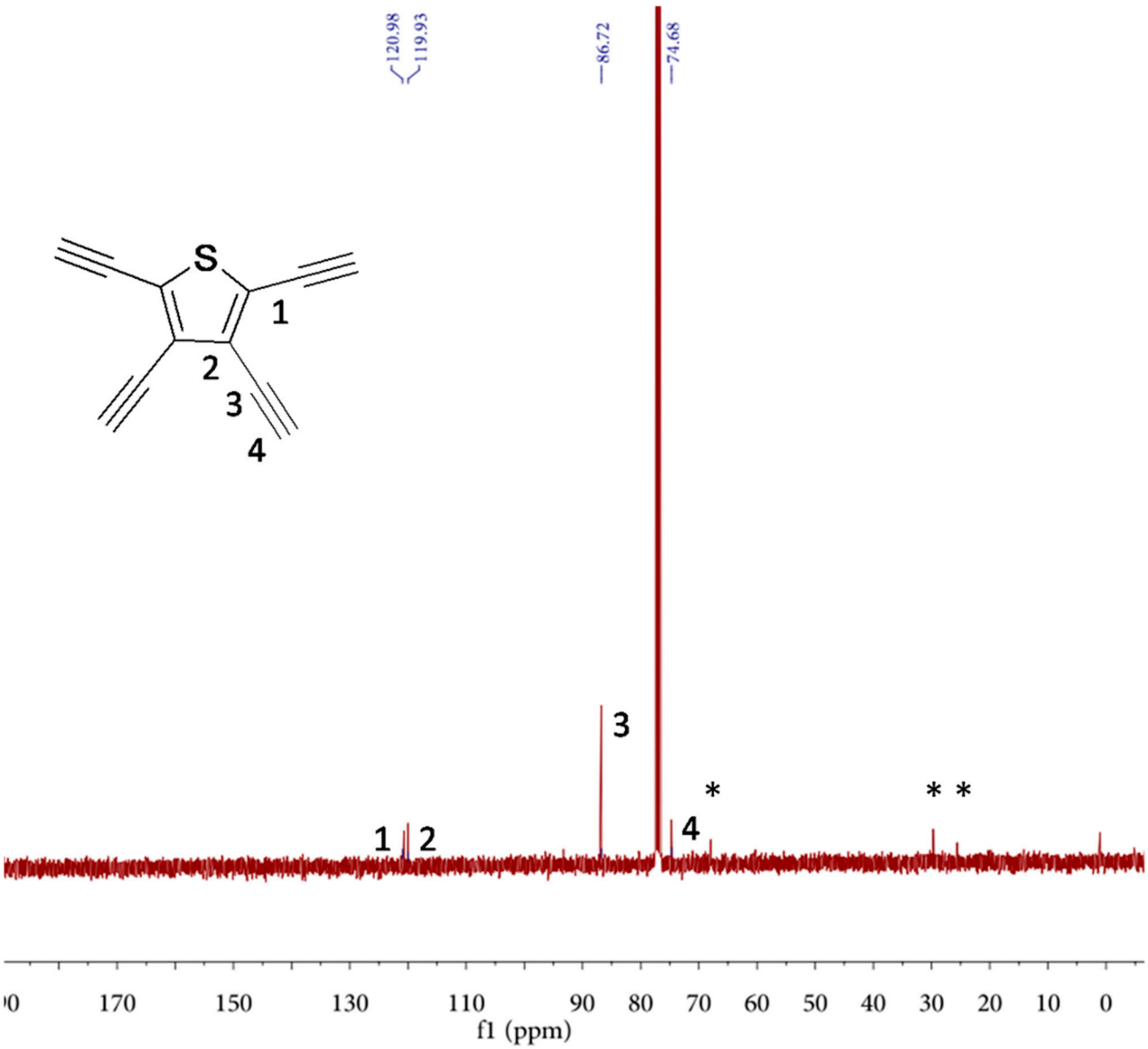

Figure S5. ^{13}C NMR spectrum of 2,3,4,5-tetraethynyl thiophene (**M1**). Attention: The NMR will be done immediately after the rotary evaporation since the monomer is unstable in the air. * may be caused by some residual solvent.

Section 2. Results of structure characterizations.

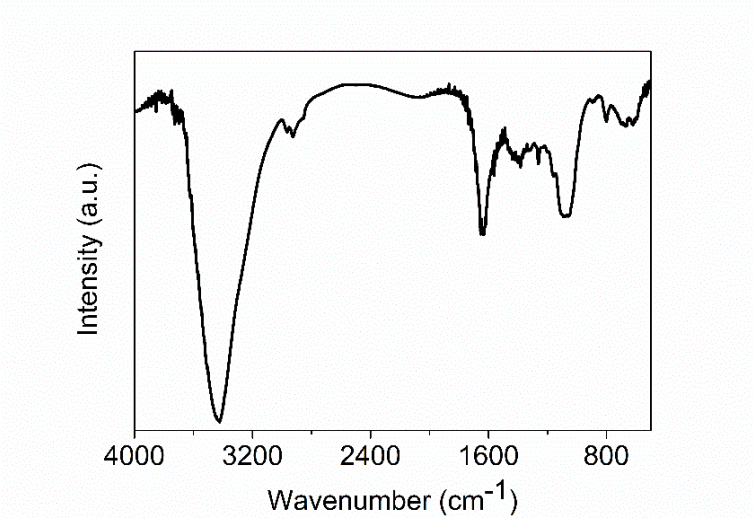

Figure S6. FT-IR spectrum of S-GDY.

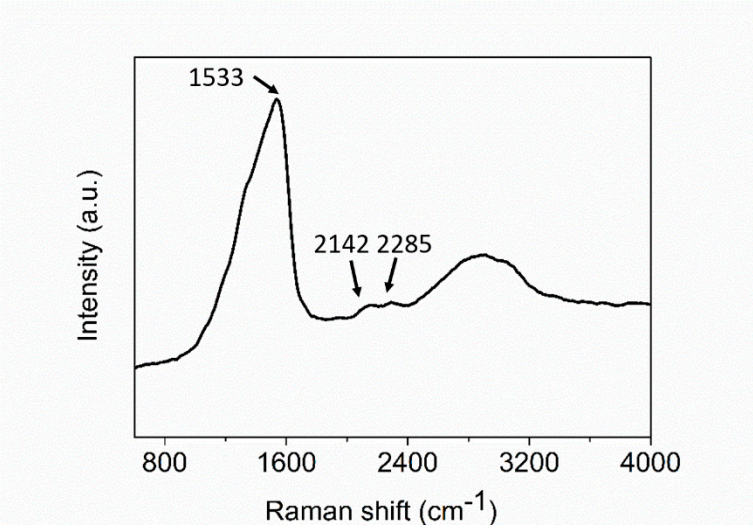

Figure S7. Raman spectrum of S-GDY.

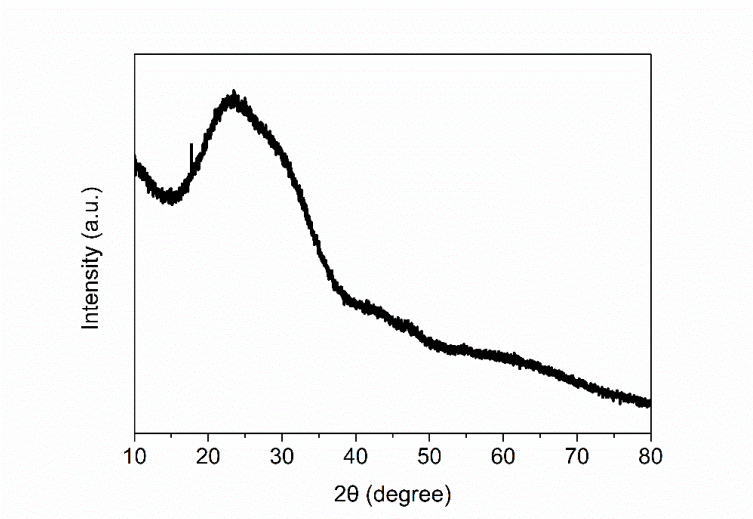

Figure S8. Power XRD pattern of S-GDY.

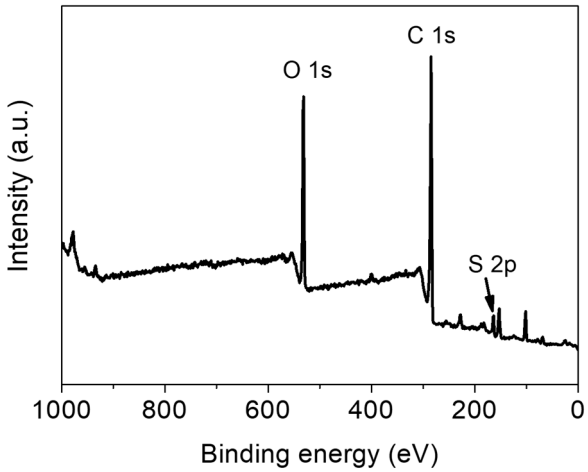

Figure S9. XPS survey spectrum of S-GDY.

Section 3. Results of porosity measurements.

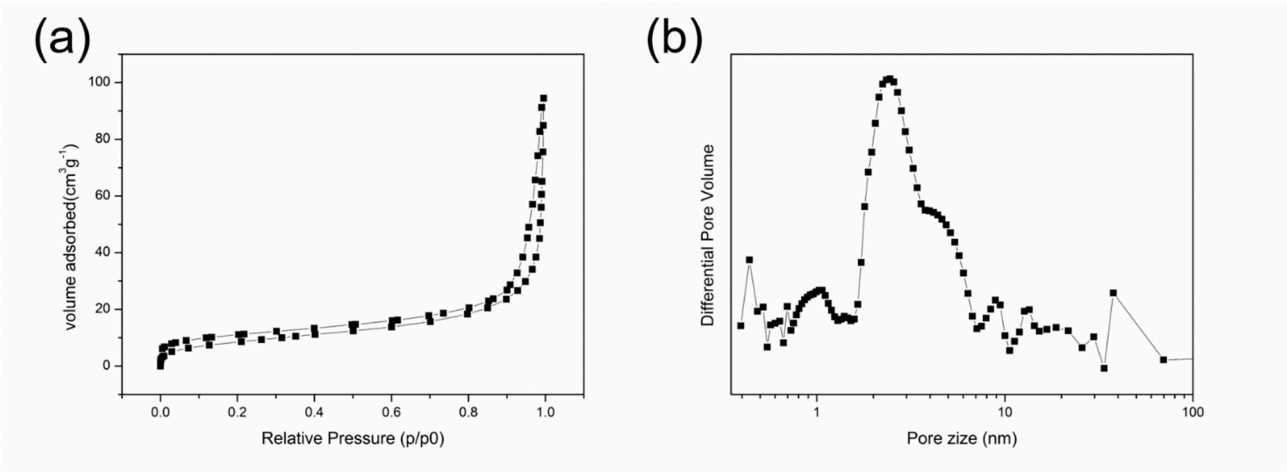

Figure S10. (**a**) Nitrogen adsorption-desorption isotherms of S-GDY, (**b**) pore size distribution profile from NLDFT calculation.

Section 4. Results of Electrochemical performances

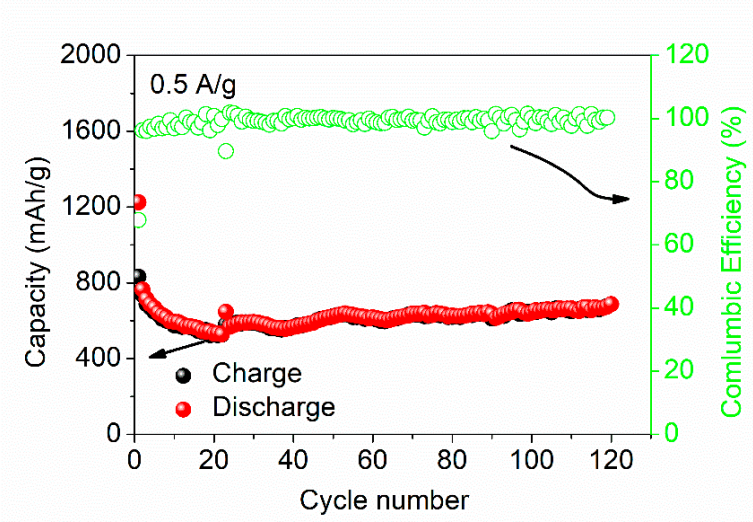

Figure S11. Long-term capacity retention at a current density of 0.5 A g^{-1}.

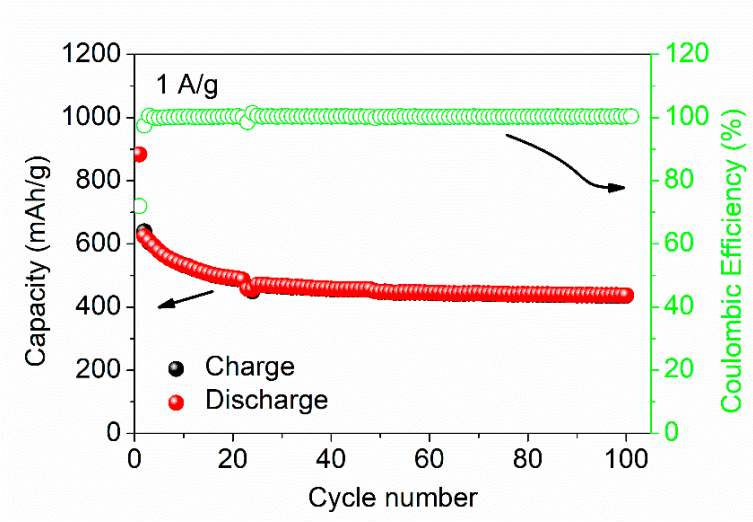

Figure S12. Long-term capacity retention at a current density of 1 A g^{-1}.

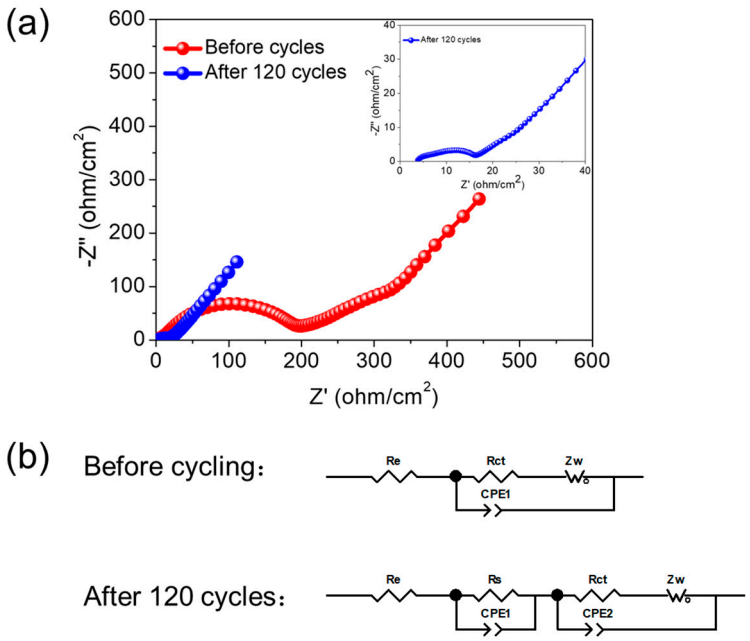

Figure S13. (**a**) Nyquist plots of the S-GDY electrode before and after 120 cycles at 0.5 A g^{-1}. The inset shows a S-GDY electrode after cycling alone in the enlarged part of the high-frequency region. (**b**) Equivalent circuits of the S-GDY electrode. In the equivalent circuit, R_e represents the electrolyte resistance; R_s is the equivalent resistance of the SEI layer formed on the electrode; R_{ct} is the charge-transfer resistance; Z_w is the Warburg impedance; CPE represents the corresponding double-layer capacitance.

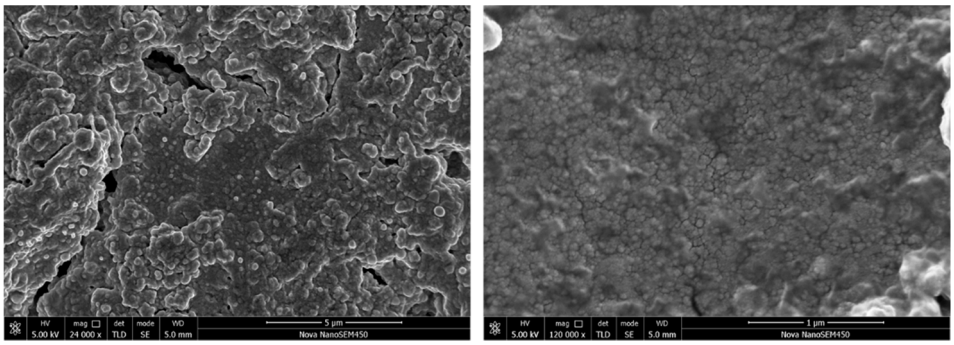

Figure S14. The SEM images of the S-GDY electrode after 120 cycles at 0.5 A g^{-1}.

Table S1. Comparison of performance of previously reported carbon-based materials.

Samples	Capacity (mA h g^{-1})	Current density (mA g^{-1})	Cycles
GDY film [1]	520	500	400
Bulk GDY [2]	552	50	200
N-GDY [3]	785	200	200
Activated carbon aerogels [4]	610	100	100
N-doped porous carbon materials [5]	488	100	100
Porous carbon [6]	833	100	50
NGY [7]	1037	100	200
S-GDY [8]	810	50	50
TTF-GDY [9]	837.6	50	200
This work	920	100	50

References

1. Huang, C.; Zhang, S.; Liu, H.; Li, Y.; Cui, G.; Li, Y. Graphdiyne for High Capacity and Long-Life Lithium Storage. *Nano Energy* **2015**, *11*, 481-489.
2. Zhang, S.; Liu, H.; Huang, C.; Cui, G.; Li, Y. Bulk Graphdiyne Powder Applied for Highly Efficient Lithium Storage. *Chem. Commun*. **2015**, *51*, 1834-1837.
3. Zhang, S.; Du, H.; He, J.; Huang, C.; Liu, H.; Cui, G.; Li, Y. Nitrogen-Doped Graphdiyne Applied for Lithium-Ion Storage. *ACS Appl. Mater. Interfaces* **2016**, *8*, 8467-8473.
4. Yang, X.; Wei, C.; Zhang, G. Activated Carbon Aerogels with Developed Mesoporosity as High-Rate Anodes in Lithium-Ion Batteries. *J. Mater. Sci.* **2016**, *51*, 5565-5571.
5. Zhang, X.; Zhu, G.; Wang, M.; Li, J.; Lu, T.; Pan, L. Covalent-Organic-Frameworks Derived N-Doped Porous Carbon Materials as Anode for Superior Long-Life Cycling Lithium and Sodium Ion Batteries. *Carbon* **2017**, *116*, 686-694.
6. Zhang, C.; Kong, R.; Wang, X.; Xu, Y.; Wang, F.; Ren, W.; Wang, Y.; Su, F.; Jiang, J.-X. Porous Carbons Derived from Hypercrosslinked Porous Polymers for Gas Adsorption and Energy Storage. *Carbon* **2017**, *114*, 608-618.
7. Yang, C.; Qiao, C.; Chen, Y.; Zhao, X.; Wu, L.; Li, Y.; Jia, Y.; Wang, S.; Cui, X. Nitrogen Doped gamma-Graphyne: A Novel Anode for High-Capacity Rechargeable Alkali-Ion Batteries. *Small* **2020**, *16*, 1907365.
8. Yang, Z.; Cui, W.; Wang, K.; Song, Y.; Zhao, F.; Wang, N.; Long, Y.; Wang, H.; Huang, C. Chemical Modification of the sp-Hybridized Carbon Atoms of Graphdiyne by Using Organic Sulfur. *Chem. - Eur. J.* **2019**, *25*, 5643-5647.
9. Pan, Q.; Chen, S.; Wu, C.; Zhang, Z.; Li, Z.; Zhao, Y. Sulfur-rich Graphdiyne-Containing Electrochemical Active Tetrathiafulvalene for Highly Efficient Lithium Storage Application. *ACS Appl. Mater. Interfaces* **2019**, *11*, 46070-46076.